MOVING FINITE ELEMENT METHOD

VLADIMIR SLADEK, MIROSLAV REPKA & JAN SLADEK
Institute of Construction and Architecture, Slovak Academy of Sciences, Slovakia

ABSTRACT
A novel discretization method is proposed and developed for numerical solution of boundary value problems governed by partial differential equations. The spatial variation of field variables is approximated by using Lagrange finite elements for interpolation without discretization of the analysed domain into the mesh of finite elements. Only the net of nodal points is used for discrete degrees of freedom on the analysed domain and its boundary. The governing equations are considered at interior nodal points while the boundary conditions at nodal points on the boundary. The finite elements are created for each nodal point properly instead of using fixed finite elements like in standard Finite Element Method. In this way, we can eliminate interfaces between elements as well as the difficulties with continuity of derivatives of field variables on such interfaces. Both the strong and weak formulations are implemented for governing equations. The reliability (accuracy and efficiency) of the new method has been verified in numerical simulations for 2D problems of heat conduction in solids with possible continuous gradation of the heat conduction coefficient.
Keywords: Lagrange finite element, bi-quadratic and bi-cubic approximation, strong and weak formulations.

1 INTRODUCTION

The Finite Element Method (FEM) is the most widely used computational method because of its universality and simplicity. Nevertheless, it suffers from discontinuities of derivatives on element interfaces as long as C^0 continuous finite elements (FE) are employed [1]. Another favourite subdomain method is the Finite Volume Method (FVM) [2], [3] enforcing the conservation (or balance) physical laws. Recently various mesh-free methods appeared which are universal. The price which should be paid for elimination of creation of discretization elements is time consuming evaluation of shape functions because of the loss of polynomial interpolation.

In 1981, Miller introduced the Moving Finite Element Method (MFEM) [5], [6] as an adaptive grid method in which the grid of finite elements deforms continuously in time with the solution. This method found wide application in vast diversity of problems in science and engineering involving time-dependent PDE describing solutions with pronounced spatial activity in some regions of space that move with time [7], [8].

In this paper, we propose the strong and weak formulations with developing the so called Moving Finite Element (MFE) approximation. In contrast to the MFEM [5]–[8], the grid of nodes is fixed (not adaptive) in the proposed method and the FE are created individually around each nodal point according to its position in the analysed domain.

2 HEAT CONDUCTION IN FGM SOLIDS: DISCRETIZATION WITH POLYNOMIAL INTERPOLATION

For the sake of simplicity, let us consider the stationary heat conduction in 2D domain of isotropic solid with the governing equation

$$\left(\lambda u_{,i}\right)_{,i} = 0 \text{ or } \lambda u_{,ii} + \lambda_{,i} u_{,i} = 0 \text{ in } \Omega \tag{1}$$

and the boundary conditions

$$u(\mathbf{x}) = T(\mathbf{x}) \text{ on } \partial\Omega_T;\ -\lambda(\mathbf{x})n_i(\mathbf{x})u_{,i}(\mathbf{x}) = f(\mathbf{x}) \text{ on } \partial\Omega_f;\ \partial\Omega = \partial\Omega_T \cup \partial\Omega_f. \quad (2)$$

The heat conduction coefficient λ is assumed to be continuous differentiable function of Cartesian coordinates. In general, the analytical solution of the mentioned boundary value problem is not available and discretization methods utilizing polynomial interpolation belong to widely spread numerical techniques because of their universality, simplicity and computational efficiency. The field variable is approximated in certain subdomain as

$$u(\mathbf{x}) = \sum_c u(\mathbf{x}^c)\varphi^c(\mathbf{x}),$$

where the unknown field variable is expressed in terms of finite number of nodal unknowns $u(\mathbf{x}^c)$ and known shape functions $\varphi^c(\mathbf{x})$. For calculation of the unknown nodal values, there are mostly used two approaches: (i) the strong formulation with collocation of the governing equation at nodal points; (ii) the weak formulation when the governing equation is considered in integral sense with using appropriate test functions. The prescribed boundary conditions can also be considered either in the strong or weak sense.

2.1 Moving Finite Element (MFE) approximation

Instead of discretization of the analysed domain into finite elements, we consider the net of nodal points which can be used for creation of so called moving finite elements individually around particular nodes according to their localization in the analysed domain as illustrated in Fig. 1 for planar elements. There are shown the bi-quadratic Lagrange elements (with 9 nodes). If $\mathbf{x}^a$ is an interior node of the analysed domain, the FE is constructed from surrounding nodes in such a way that $\mathbf{x}^a$ is the centre of the FE. In the case of a corner node the associated FE is constructed uniquely. Finally, the FE associated with other boundary node involves this node as the mid-side node of the FE. Obviously, a uniform mesh of nodes is the most appropriate one for generation of moving finite elements around each node. Having defined the FE around particular nodes $\mathbf{x}^a$, one can simply approximate the spatial variation of a field variable within the associated moving finite element E^a

$$u(\mathbf{x})\big|_{E^a} \approx \sum_{\gamma=1}^{n} u^{a_\gamma} N^\gamma(\boldsymbol{\xi}),\ u^{a_\gamma} = u(\mathbf{x}^{a_\gamma}), \quad (3)$$

where $\boldsymbol{\xi}$ is the shortcut for intrinsic coordinates (ξ_1, ξ_2), $N^\gamma(\boldsymbol{\xi})$ stand for standard interpolation shape functions in Lagrange FE, and a_γ is the global number of the node on the element E^a with the local number $\gamma \in \{1, 2, ..., n\}$. In order to account also the 2nd order derivatives of field variables, it is necessary to use finite elements with complete higher order polynomial interpolation, at least bi-quadratic Lagrange FE defined with 9 nodes [1].

If $\mathbf{x}^a$ is an interior node of the analysed domain, the FE is constructed from surrounding nodes in such a way that $\mathbf{x}^a$ is the centre of the FE. In the case of a corner node the associated FE is constructed uniquely. Finally, the FE associated with other boundary node involves this node as the mid-side node of the FE. Obviously, a uniform mesh of nodes is the most

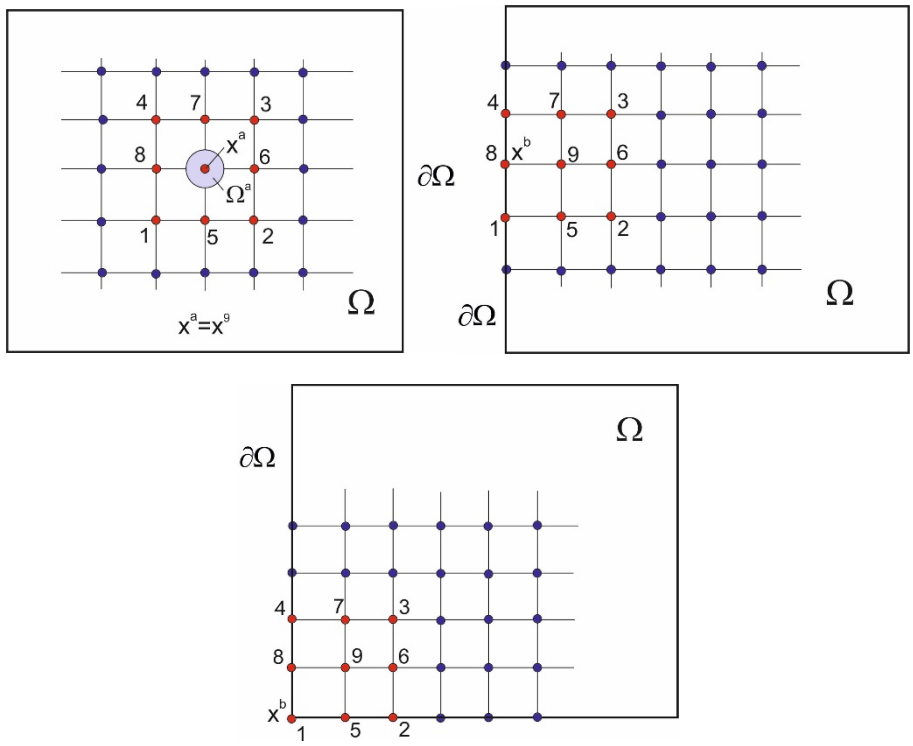

Figure 1: Creation of moving FE around the interior node $\mathbf{x}^a$ as well as the boundary node and corner nodes $\mathbf{x}^b$.

appropriate one for generation of moving finite elements around each node. Having defined the FE around particular nodes $\mathbf{x}^a$, one can simply approximate the spatial variation of a field variable within the associated moving finite element E^a

$$u(\mathbf{x})\big|_{E^a} \approx \sum_{\gamma=1}^{n} u^{a_\gamma} N^\gamma(\boldsymbol{\xi}),\ u^{a_\gamma} = u(\mathbf{x}^{a_\gamma}), \tag{3}$$

where $\boldsymbol{\xi}$ is the shortcut for intrinsic coordinates (ξ_1, ξ_2), $N^\gamma(\boldsymbol{\xi})$ stand for standard interpolation shape functions in Lagrange FE, and a_γ is the global number of the node on the element E^a with the local number $\gamma \in \{1, 2, ..., n\}$. In order to account also the 2nd order derivatives of field variables, it is necessary to use finite elements with complete higher order polynomial interpolation, at least bi-quadratic Lagrange FE defined with 9 nodes [1]. The gradient of the field variable can be approximated on the FE as

$$u_{,i}(\mathbf{x})\big|_{E^a} = \left.\frac{\partial u(\mathbf{x})}{\partial x_i}\right|_{E^a} \approx \sum_{\gamma=1}^{n} u^{a_\gamma} b_i^{\gamma a}(\boldsymbol{\xi}),\ b_i^{\gamma a}(\boldsymbol{\xi}) = \mathrm{Y}_{ik}^a \frac{\partial N^\gamma(\boldsymbol{\xi})}{\partial \xi_k},\ \mathrm{Y}_{ik}^a = \left.\frac{\partial \xi_k}{\partial x_i}\right|_{E^a}, \tag{4}$$

Recall that the matrix $[\mathrm{Y}^a]$ is the inverse of the Jacobi matrix, i.e. $[Y^a]=[J^a]^{-1}$, and

$$\left[J^a\right]=\begin{pmatrix}\partial x_1/\partial\xi_1 & \partial x_2/\partial\xi_1\\ \partial x_1/\partial\xi_2 & \partial x_2/\partial\xi_2\end{pmatrix}\Bigg|_{E^a}=\sum_{\gamma=1}^{n}\begin{pmatrix}x_1^{a_\gamma}\partial N^\gamma/\partial\xi_1 & x_2^{a_\gamma}\partial N^\gamma/\partial\xi_1\\ x_1^{a_\gamma}\partial N^\gamma/\partial\xi_2 & x_2^{a_\gamma}\partial N^\gamma/\partial\xi_2\end{pmatrix},$$

$$J^a_{ki}=\left.\frac{\partial x_i}{\partial\xi_k}\right|_{E^a}=\sum_{\gamma=1}^{n}x_i^{a_\gamma}\frac{\partial N^\gamma}{\partial\xi_k}, \tag{5}$$

since we use the isoparametric elements and the Cartesian coordinates are approximated as

$$x_i\big|_{E^a}\approx\sum_{\gamma=1}^{n}x_i^{a_\gamma}N^\gamma(\boldsymbol{\xi}). \tag{6}$$

Apparently,

$$\left[Y^a\right]=\left[J^a\right]^{-1}=\frac{1}{\left|J^a\right|}\sum_{\beta=1}^{n}\begin{pmatrix}x_2^{a_\beta}\partial N^\beta/\partial\xi_2 & -x_2^{a_\beta}\partial N^\beta/\partial\xi_1\\ -x_1^{a_\beta}\partial N^\beta/\partial\xi_2 & x_1^{a_\beta}\partial N^\beta/\partial\xi_1\end{pmatrix},$$

$$\left|J^a\right|=\left(\frac{\partial x_1}{\partial\xi_1}\frac{\partial x_2}{\partial\xi_2}-\frac{\partial x_1}{\partial\xi_2}\frac{\partial x_2}{\partial\xi_1}\right)\Bigg|_{E^a}=\sum_{\alpha,\beta=1}^{n}x_1^{a_\alpha}x_2^{a_\beta}\left(\frac{\partial N^\alpha}{\partial\xi_1}\frac{\partial N^\beta}{\partial\xi_2}-\frac{\partial N^\alpha}{\partial\xi_2}\frac{\partial N^\beta}{\partial\xi_1}\right). \tag{7}$$

As regards the 2nd order derivatives, we can write

$$u_{,ij}(\mathbf{x})\big|_{E^a}=\left.\frac{\partial^2u(\mathbf{x})}{\partial x_i\partial x_j}\right|_{E^a}\approx\sum_{\gamma=1}^{n}u^{a_\gamma}\frac{\partial\xi_m}{\partial x_j}\frac{\partial}{\partial\xi_m}b_i^{\gamma a}(\boldsymbol{\xi})=$$

$$=\sum_{\gamma=1}^{n}u^{a_\gamma}Y^a_{jm}\frac{\partial}{\partial\xi_m}\left(Y^a_{ik}N^\gamma_{,k}(\boldsymbol{\xi})\right)=\sum_{\gamma=1}^{n}u^{a_\gamma}Y^a_{jm}\left[Y^a_{ik}N^\gamma_{,km}(\boldsymbol{\xi})+Y^a_{ik,m}N^\gamma_{,k}(\boldsymbol{\xi})\right]=$$

$$=\sum_{\gamma=1}^{n}u^{a_\gamma}Y^a_{jm}\left[Y^a_{ik}N^\gamma_{,km}(\boldsymbol{\xi})-Y^a_{is}J^a_{sl,m}Y^a_{lk}N^\gamma_{,k}(\boldsymbol{\xi})\right]=$$

$$=\sum_{\gamma=1}^{n}u^{a_\gamma}Y^a_{jm}\left[Y^a_{ik}N^\gamma_{,km}(\boldsymbol{\xi})-Y^a_{is}J^a_{sl,m}b_l^{\gamma a}(\boldsymbol{\xi})\right]=\sum_{\gamma=1}^{n}u^{a_\gamma}b_{ij}^{\gamma a}(\boldsymbol{\xi}) \tag{8}$$

since

$$\left(Y^a_{ik}J^a_{kl}\right)_{,m}=0=Y^a_{ik,m}J^a_{kl}+Y^a_{ik}J^a_{kl,m}\;\Rightarrow\;Y^a_{ik,m}=-Y^a_{is}J^a_{sl,m}Y^a_{lk}$$

$$\text{with } J^a_{sl,m} = \sum_{\gamma=1}^{n} x_l^{a_\gamma} \frac{\partial^2 N^\gamma}{\partial\xi_s \partial\xi_m} = J^a_{ml,\mathrm{s}}$$

$$b^{\gamma a}_{ij}(\boldsymbol{\xi}) := Y^a_{jm}\left[Y^a_{ik} N^\gamma_{,km}(\boldsymbol{\xi}) - Y^a_{is} J^a_{sl,m} b^{\gamma a}_l(\boldsymbol{\xi}) \right] = b^{\gamma a}_{ji}(\boldsymbol{\xi}) . \tag{9}$$

Note that in the case of standard FEM with C^0 continuous elements, one can expect discontinuities of both the 1st and 2nd order derivatives on interfaces of finite elements. On the other hand, in the case of moving finite elements approximation, there are no element interfaces because each node is either interior node of the associated FE, or it is a mid-side node or a corner of the associated FE. Thus, the C^0-continuity troubles of standard FEM disappear in formulations based on MFE approximation.

2.2 Strong formulation based of MFE approximation

The strong formulation seems to be computationally the most efficient formulation because the only thing, needed for creation of discretized equations for calculation of nodal unknowns, is approximation of derivatives at nodal points, since the discretized equations take the form

$$\lambda(\mathbf{x}^c) \sum_{\gamma=1}^{n} u^{c_\gamma} b^{\gamma c}_{ij}(\boldsymbol{\xi}^{\alpha_c}) + \lambda_{,i}(\mathbf{x}^c) \sum_{\gamma=1}^{n} u^{c_\gamma} b^{\gamma c}_{i}(\boldsymbol{\xi}^{\alpha_c}) = 0 \text{ for each } \mathbf{x}^c \in \Omega , \tag{10a}$$

$$u(\mathbf{x}^b) = T(\mathbf{x}^b) \text{ for } \mathbf{x}^b \in \partial\Omega_T , \tag{10b}$$

$$\lambda n_i(\mathbf{x}^b) \sum_{\gamma=1}^{n} u^{b_\gamma} b^{\gamma b}_{i}(\boldsymbol{\xi}^{\alpha_b}) = -f(\mathbf{x}^b) \text{ for } \mathbf{x}^b \in \partial\Omega_f , \tag{10c}$$

where α_c is the local number (and $\xi_1^{\alpha_c}$, $\xi_2^{\alpha_c}$ are intrinsic coordinates) of the global node $\mathbf{x}^c$ on the associated finite element E^c. The formulation resembles the Finite Difference Method (FDM), but the approximation of field variable used here is different.

2.3 Weak formulation based of MFE approximation

The weak form of the governing eqn (1) is given as

$$\int_\Omega \left(\lambda(\mathbf{x}) u_{,i}(\mathbf{x}) \right)_{,i} \omega(\mathbf{x}) d\Omega = 0 , \tag{11}$$

where $\omega(\mathbf{x})$ is a weight function. Selecting the weight function as the compactly supported function

$$\omega^a(\mathbf{x}) = \begin{cases} 1, & \mathbf{x} \in \overline{\Omega}^a , \\ 0, \text{ otherwise}, \end{cases}$$

with $\overline{\Omega}^a = \Omega^a \cup \partial\Omega^a$ being the subdomain of the analysed domain $\overline{\Omega}$ and taken around a point $\mathbf{x}^a \in \overline{\Omega}^a \subset \overline{\Omega}$, eqn (11) can be rewritten as

$$\int_{\partial\Omega^a} n_i(\mathbf{x})\lambda(\mathbf{x})u_{,i}(\mathbf{x})d\Omega = 0\,, \tag{12}$$

where $n_i(\mathbf{x})$ is the unit outward normal vector at $\mathbf{x} \in \partial\Omega^a$.

From the physical point of view, eqn (12) expresses the energy balance in local subdomain $\overline{\Omega}^a$ with absent volume heat sources. From the mathematical point of view, it is the formulation for solution of the considered problem by the Finite Volume Method (FVM) [4] without specifying the approximation of field variable. In this paper, we employ the MFE for approximation. In contrast to the strong formulation, now it is sufficient to approximate only the 1st order derivatives of the field variable, but we need to integrate over the boundary of local subdomain. Recall that the subdomain $\overline{\Omega}^a$ should involve only one nodal point $\mathbf{x}^a$ in the assumed MFE approximation. Since there are no other restrictions for selection of $\overline{\Omega}^a$, it is reasonable to select such a shape of $\overline{\Omega}^a$ that the integration over $\partial\Omega^a$ would be as simple as possible. Furthermore, the integration is carried out in the intrinsic space and Ω^a is the image of $\tilde{\Omega}^a$ resulting from the transformation: $\tilde{\Omega}^a \ni \boldsymbol{\xi} \to \mathbf{x} \in \Omega^a$ according to (6). Therefore we select $\tilde{\Omega}^a$ as the circle centred at $\left(\xi_1^{\alpha_a}, \xi_2^{\alpha_a}\right)$, i.e. $\tilde{\Omega}^a = \left\{\forall\, \boldsymbol{\xi} \in \tilde{E}^a;\, |\boldsymbol{\xi} - \boldsymbol{\xi}^{\alpha_a}| < 1\right\}$. Denoting the radius of the circular contour $\partial\tilde{\Omega}^a$ as ξ^a, the intrinsic coordinates of a point on $\partial\tilde{\Omega}^a$ can be expressed in terms of one angular parameter $\varphi \in [0,\, 2\pi]$ as

$$\partial\tilde{\Omega}^a = \left\{\forall\, \boldsymbol{\xi} \in \tilde{E}^a;\, \xi_k = \xi_k^{\alpha_a} + \xi^a\left(\delta_{k1}\cos\varphi + \delta_{k2}\sin\varphi\right)\right\}. \tag{13}$$

Since ξ^a is constant on $\partial\tilde{\Omega}^a$, we have $d\xi_k\big|_{\partial\tilde{\Omega}^a} = \xi^a\tilde{\tau}_k d\varphi$, $\tilde{\tau}_k = \delta_{k2}\cos\varphi - \delta_{k1}\sin\varphi$ and the infinitesimal length arc of circular contour $\partial\tilde{\Omega}^a$ is $ds\big|_{\partial\tilde{\Omega}^a} = \tilde{\tau}_k d\xi_k = \xi^a d\varphi$. Then,

$$d\Gamma\big|_{\partial\Omega^a} = \tau_i dx_i\big|_{\partial\Omega^a} = \tau_i \frac{dx_i}{ds}ds\bigg|_{\partial\Omega^a} = \frac{g_i}{g}g_i ds\bigg|_{\partial\Omega^a} = g\big|_{\partial\Omega^a}\xi^a d\varphi\,, \tag{14}$$

where the unnormalized tangent vector on $\xi_2^{\alpha_a}$ $\partial\Omega^a$ is defined as $g_i := dx_i / ds$ and it can be expressed as

$$g_i\big|_{\partial\Omega^a} = \frac{1}{\xi^a}\frac{dx_i}{d\varphi}\bigg|_{\partial\Omega^a} = \frac{1}{\xi^a}\frac{\partial x_i}{\partial\xi_j}\frac{\partial\xi_j}{d\varphi}\bigg|_{\partial\Omega^a} = \frac{1}{\xi^a}\left(\frac{\partial x_i}{\partial\xi_2}\cos\varphi - \frac{\partial x_i}{\partial\xi_1}\sin\varphi\right)\bigg|_{\partial\Omega^a}.$$

Hence,

$$g_i^{\partial\Omega^a} := g_i\big|_{\partial\Omega^a} = \frac{1}{\xi^a}\sum_{\gamma=1}^{n} x_i^{a_\gamma}\left(N_{,2}^{\gamma}(\boldsymbol{\xi}^{\partial\Omega^a})\cos\varphi - N_{,1}^{\gamma}(\boldsymbol{\xi}^{\partial\Omega^a})\sin\varphi\right), \tag{15}$$

with $\boldsymbol{\xi}^{\partial\Omega^a} := \left(\xi_1^{\partial\Omega^a}, \xi_2^{\partial\Omega^a}\right) = \left(\xi_1^{\alpha_a}, \xi_2^{\alpha_a}\right) + \xi^a\left(\cos\varphi, \sin\varphi\right)$.

The unit normal vector on $\partial\Omega^a$ can be defined as $n_i\big|_{\partial\Omega^a} = \varepsilon_{ik3} g_k^{\partial\Omega^a} / g^{\partial\Omega^a}$. Thus, eqn (12) can be rewritten as

$$\varepsilon_{ik3}\xi^a \sum_{\gamma=1}^{n} u^{a_\gamma} \int_0^{2\pi} \lambda(\mathbf{x}^{\partial\Omega^a}) b_i^{\gamma a}(\boldsymbol{\xi}^{\partial\Omega^a}) g_k^{\partial\Omega^a} d\varphi = 0, \tag{16}$$

with the Cartesian coordinates of the integration point on $\partial\Omega^a$ are given by

$$x_i^{\partial\Omega^a} := x_i\big|_{\partial\Omega^a} = \sum_{\gamma=1}^{n} x_i^{a_\gamma} N^{\gamma}(\boldsymbol{\xi}^{\partial\Omega^a}).$$

The discretized prescribed boundary conditions can be considered in the same way as in the strong formulation. Then, the complete set of discretized equations in the weak formulation is given by eqns (16), (10b) and (10c).

3 NUMERICAL EXAMPLES

In order to test the applicability of the MFE approximation, we compared accuracy and computational efficiency achieved by both the strong and weak formulations with MFE approximation and by the standard FEM in solving simple problem of stationary heat conduction in a rectangular domain of solids with constant and/or functionally graded heat conduction coefficient λ. The dimensionless formulation is used with $L_1 \times L_2 = 3 \times 3$, prescribed temperature on the bottom and top $u(x_1, x_2 = 0) = 0$, $u(x_1, x_2 = 3) = 100$; the lateral sides are thermally isolated $n_i u_{,i}\big|_{x_1=0} = 0 = n_i u_{,i}\big|_{x_1=3}$; the functional gradation is considered as power-law gradation in the vertical direction $\lambda = \lambda_0\left(1 + 2x_2 / L_2\right)^2$. In numerical solution, we employed uniform net of nodal points with n_1, n_2, $N = n_1 \times n_2$ being the number of nodes in horizontal and vertical directions, and the total number of nodes, respectively. Since we shall use also the standard FEM, the net of nodes is designed to be applicable also to FEM discretization. Furthermore, the Lagrange finite element is composed of $\sqrt{n} \times \sqrt{n}$ nodes. Therefore, $n_1 = e_1\left(\sqrt{n} - 1\right)$ and $n_2 = e_2\left(\sqrt{n} - 1\right)$, where e_k is the number of FE along the x_k -direction. Since the problem is actually 1-dimensional, we have chosen $e_1 = 1$ and e_2 (or n_2) to be variable. Finally, we have used quadrilateral bi-quadratic ($n = 9$) as well as bi-cubic ($n = 16$) Lagrange finite elements. The accuracy is characterized by average relative error defined as

$$\frac{1}{N}\sum_{a=1}^{N}\left|\frac{f^c(\mathbf{x}^a)}{f^e(\mathbf{x}^a)}-1\right|,$$

with the superscripts c and e denoting the computed and exact values, respectively.

Firstly, consider the results for heat conduction in a homogeneous solid. We achieved very precise numerical results for the temperature $u^c(\mathbf{x})$ as well as temperature gradients $u^c_{,2}(\mathbf{x})$. In this case, the exact solution is given by linear distribution of temperature and almost exact solution is achieved by using only one FE. Any other increase of degrees of freedom in numerical calculation yields increasing numerical error. Nevertheless, the best accuracy is achieved by strong formulations with MFE approximation. Since $u^e_{,22}(\mathbf{x}) \equiv 0$, we have used average absolute error instead of average relative error. Now, the accuracy by standard FEM is significantly worse than that by using formulations with MFE approximation and the bi-cubic FE results into one order better accuracy than the bi-quadratic FE.

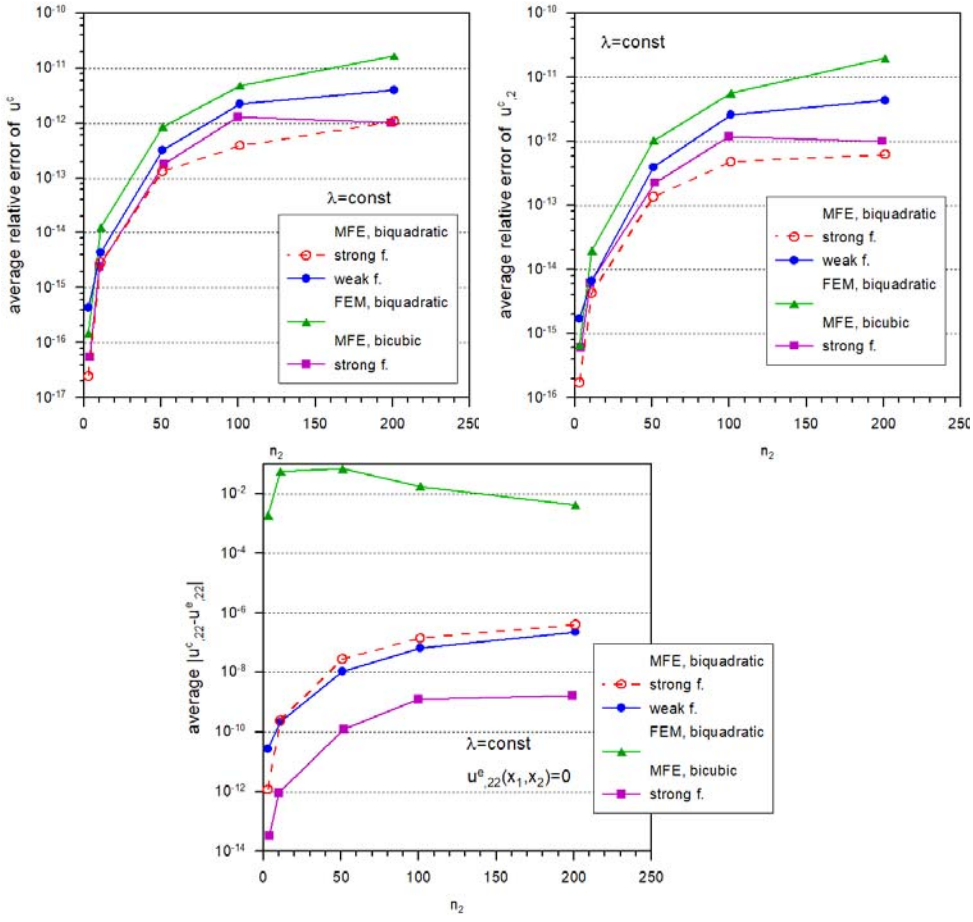

Figure 2: Comparison of accuracies for u^c, $u^c_{,2}$, and $u^e_{,22}$ in a homogeneous solid.

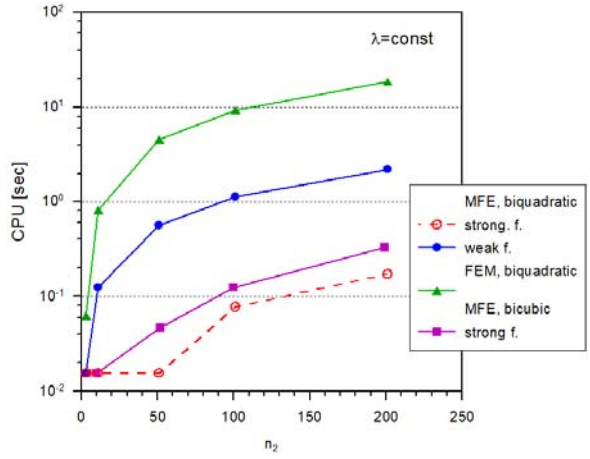

Figure 3: Comparison of computational efficiency in case of homogeneous solid.

There is significant difference between the computational times by using standard FEM and formulations with MFE as well as between the strong and weak formulations.

Substantially different accuracy is achieved for problems in FGM solid, when the exact solution exhibits a non-linear variation. Unexpectable accurate are numerical results for u^c obtained by strong formulation with MFE approximation. The other three techniques exhibit convergence to exact solution with increasing the amount of nodes and the convergence of u^c by the standard FEM is faster than by other two MFE approaches. Nevertheless, the best accuracy of $u^c_{,2}$ is achieved by the MFE with bi-cubic FE, while in the case of bi-quadratic FE there is no difference in accuracy achieved by the weak and strong formulations with MFE and the accuracy by standard FEM is the worst. Similar conclusion can be drawn also for the accuracy of $u^e_{,22}$ but the differences in achieved values are more remarkable. As regards the computational times, these are practically the same as in the case of homogeneous solid. The main shortcoming of the standard FEM approach consists in discontinuity of derivatives on FE interfaces. The differences in relative errors of $u^c_{,2}$ vary between 3% (on the top of bottom FE) and 0.5% (on the bottom of the top FE) if $e_2 = 5$, while in the case of $u^e_{,22}$ these differences are 28% and 6%.

4 CONCLUSIONS

The Moving Finite Element (MFE) approximation is proposed and developed. In contrast to the standard FEM, there is no mesh of FE created, but the polynomial interpolation is successfully utilized within MFE created individually around each nodal point of the net of nodes. Thus, the difficulty of discontinuous derivatives on FE interfaces is eliminated and C^0 continuous Lagrange FE are applicable to both the weak and strong formulations for solution of boundary value problems. In numerical test examples, the reliability of the method is verified and comparative study accomplished with using quadrilateral bi-quadratic and bi-cubic Lagrange FE.

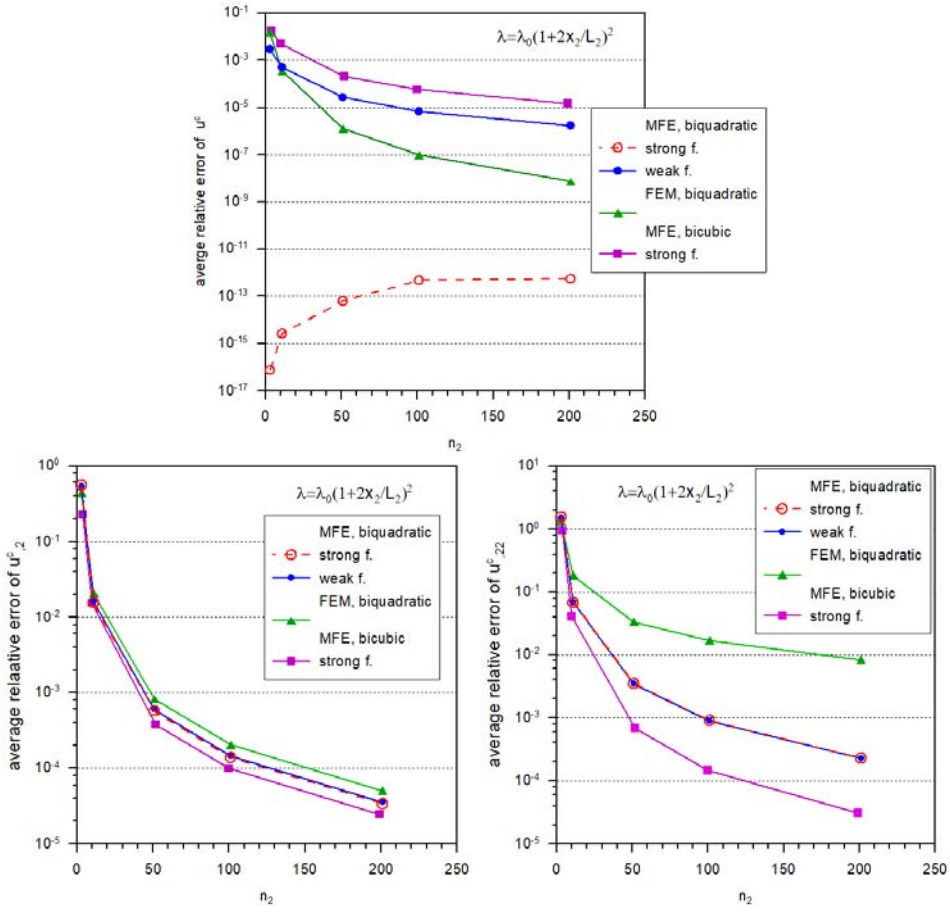

Figure 4: Comparison of accuracies for u^c, $u^c_{,2}$, and $u^e_{,22}$ in the FGM solid.

ACKNOWLEDGEMENT

This work was partially supported by the Slovak Research and Development Agency under the contract No. APVV-14-0440.

REFERENCES

[1] Hughes, T.J.R., *The Finite Element Method, Linear Static and Dynamic Finite Element Analysis*, Prentice-Hall, Inc.: Englewood Cliffs, 1987.

[2] McDonald, P.W., The computation of transonic flow through two-dimensional gas cascades. *ASME 1971 International Gas Turbine Conference and Products Show*, pp. V001T01A089, 1971. DOI:10.1115/71-GT-89.

[3] MacCormack, R.W. & Paullay, A.J., Computational efficiency achieved by time splitting of finite difference operators. *AIAA paper,* pp. 72–154, 1972.

[4] Kolditz, O., *Computational Methods in Environmental Fluid Mechanics, Chapter 8: Finite Volume Method*, Springer-Verlag: Heidelberg, pp. 173–190, 2002.

[5] Miller, K. & Miller, R., Moving finite elements I. *SIAM Journal Numerical Analysis,* **18**(6), pp. 1019–1032, 1981.
[6] Miller, K., Moving finite elements II. *SIAM Journal Numerical Analysis,* **18**(6), pp. 1033–1057, 1981.
[7] Coimbra, M., Rodrigues, A., Rodrigues, J., Robalo, R. & Almeida, R., *Moving Finite Element Method, Fundamentals and Applications in Chemical Engineering*, CRC Press: Boca Raton, 2016.
[8] Baines, M., Hubbard, M., Jimack, P. & Mahmood, R., A moving-mesh finite element method and its application to the numerical solution of phase-change problems. *Communications in Computational Physics*, **6**, pp. 595–624, 2009.